Applied Energy 285 (2021) 116399

Contents lists available at ScienceDirect

Applied Energy

journal homepage: www.elsevier.com/locate/apenergy

Multi-level trading community formation and hybrid trading network construction in local energy market

Li Ma, Lingfeng Wang *, Zhaoxi Liu

Department of Electrical Engineering and Computer Science, University of Wisconsin-Milwaukee, Milwaukee, WI 53211, USA

A R T I C L E I N F O

Keywords:
Local energy trading
Trading community formation
Hybrid trading network
P2P trading
Agent-based trading

A B S T R A C T

Community-based trading structures play important roles in the development of local energy market (LEM). In this paper, a decentralized optimization model for the trading community formation is proposed based on the Lp-box consensus alternating direction method of multipliers (ADMM), where the network features of the physical systems are explicitly represented by power loss and wheeling charging in local and regional trading level, respectively. The framework for multi-level hybrid trading network construction is introduced involving three different trading modes, *i.e*, traditional trading mode, agent-based trading mode and peer-to-peer (P2P) trading mode, and two hybrid trading networks, namely Traditional trading & Agent based trading (TA) and Traditional trading & Peer-to-peer trading & Agent based trading (TPA), are developed based on the trading community formation results. The corresponding profit allocation schemes are also presented for the TA and TPA hybrid trading networks respectively. A set of complex network indices is applied to analyze the network characteristics of the TA and TPA trading topologies, while the link entropy (LE) index is used to evaluate the edge significance of the communication relationship network in maintaining global connectivity. Finally, the proposed models are validated via a test system with six IEEE 33-bus systems connected through the IEEE 9-bus system. The results show that the agent-based strategy can benefit all entities compared with the SDR and contribution-based strategies, while the REO (renewable energy output)-first strategy proposed for P2P pairing is more stimulating for the selling entities with larger REOs than distance-first mode. In addition, the entities' prices in the bi-level trading are significantly improved compared with those of the single-level trading both for agent-based trading and P2P trading. The complex index values of TA are all slightly greater than those of TPA, and a feeder with fewer managers is likely to have a larger LE value. The proposed models for trading community formation and trading network formation provide significant means for the development of sustainable LEMs.

1. Introduction

Concerns on environmental problems [1] and energy supply security have arisen over the past decades due to the fast dwindling natural resources and rapid increase of fossil fuel demand. As a potential solution to these concerns, renewable energy-based distributed generations (DGs), *i.e.*, localized or on-site power generation, have been widely deployed in the distribution network along with a steady price decrease of small-scale renewable generators [2].

The proliferation of customer-owned DGs (mainly based on renewable energy sources (RES)) is transforming the electricity consumers to the so-called prosumers (*i.e.*, consumers with the ability to generate electricity). However, most prosumers who have local energy generation still can only trade with the utility companies because of the barriers from the wholesale market, such as capacity barrier to market entry, vulnerability to cyberattacks, and limited extensibility of the centralized structure [3]. As a result, they either purchase energy from or sell surplus energy back to the utilities directly while suffering from some prices gap [4]. With prosumers increasing in number, they will most likely demand a market for a higher degree of freedom in energy trading [5], which would bring more profits to the prosumers. From the viewpoint of utility grid, massive access of DGs based on intermittent renewable energy will bring about great challenges to the power system as the utility grid was not designed for a bidirectional power flow essentially. In some cases, the output of the DGs cannot be fully utilized due to the capacity constraints of the power grid. In addition, with the rapid growth of power consumption, including the new forms of loads such as electric vehicles and non-fossil-based heating, the utility grid needs upgrades and reconstruction, which are highly costly. The local balance of demand and DG in the distribution system is a promising strategy to mitigate the abovementioned problems.

* Corresponding author.
E-mail addresses: ma27@uwm.edu (L. Ma), l.f.wang@ieee.org (L. Wang), zhaoxil@uwm.edu (Z. Liu).

https://doi.org/10.1016/j.apenergy.2020.116399
Received 10 September 2020; Received in revised form 4 December 2020; Accepted 23 December 2020
0306-2619/© 2020 Elsevier Ltd. All rights reserved.

Nomenclature

Parameter

C^t_{whp}	The wheeling charge in the pth regional community at period t.
c_i	The communities to which vertex i is assigned.
c_j	The communities to which vertex j is assigned.
d_{ik}	Distance between manager i and entity k in local trading level.
d_{ave}	Average distance (between two entities) in the whole distribution feeder.
n_l	The number of lines in transmission network.
N_M	Number of managers in the regional trading.
N_E	Number of entities in the regional trading.
n_m	Number of managers in the general model.
n_e	Number of entities in the general model.
n_{mf}	Number of managers in the fth feeder's local trading.
n_{ef}	Number of entities in the fth feeder's local trading.
P^t_k	Load of the kth local entity at period t. (For the selling entity, the value is negative)
$P_{loss^t_i}$	Power loss in the ith local community at period t.
P^t_q	Load of the qth regional entity at period t. (For the selling entity, the value is negative)
P^t_{ik}	Load of the kth local entity taking part in the ith local community at period t.
P^t_{pq}	Load of the qth regional entity taking part in the pth regional community at period t.
p	The natural number in Lp-box intersection.
p^t_s	Selling price of the utility grid at period t.
p^t_b	Buying price of the utility grid at period t.
p^t_{wh}	Wheeling charge per megawatt (MW) on the transmission line.
r_{loss}	Average power loss rate in the distribution network.
V^t_i	Trading volume in the ith local community at period t.
V^t_p	Trading volume in the pth regional community at period t.
X_{ij}	The reactance of the line with endnodes i and j.
ρ	Correction factor considering DGs.
$\rho_1 \sim \rho_4$	The positive penalty parameters.

Matrix & Vector

$\mathbf{1}_n$	An n-dimensional vector with all elements equal to 1.
A	The adjacent matrix for a graph.
$\mathbf{E}_n$	An n-dimensional unit matrix.
$\boldsymbol{Pin}^t_{pq}$	The injecting power vector (column vector) corresponding to the trade between regional community p and regional entity q.
$\boldsymbol{PTDF}_l$	The lth row in the matrix PTDF.
$\boldsymbol{S}_b$	An n-dimensional box $[0,1]^n$ with unit length.
$\boldsymbol{S}_p$	An $(n-1)$-dimensional sphere with center at $\frac{1}{2}\mathbf{1}_n$ and radius $(n^{\frac{1}{p}}/2)$.

Variable

x_{ijk}	The element in $\boldsymbol{x}_i$, x_{ijk}=1 when the kth entity will join manager j's community in the variables of manager i, otherwise $x_{ijk}=0$.
$y_{1i} \sim y_{4i}$	The dual variables in Lp-box ADMM model.

Acronym

ACC	Average clustering coefficient
AD	Average degree
ADMM	Alternating direction method of multipliers
APL	Average path length
AWD	Average weighted degree
CN	Complex network
DG	Distributed generations
ICT	Information and communication technology
LE	Link entropy
LEM	Local energy market
MMR	Mid-market rate
P2P	Peer-to-peer
PV	Photovoltaics
PTDF	Power transfer distribution factor
REO	Renewable energy output
RES	Renewable energy sources
SDR	Supply and demand ratio
TA	Traditional trading & Agent-based trading
TM	Trading manager
TPA	Traditional trading & Peer-to-peer trading & Agent-based trading

Under this background, the local energy market (LEM), which is a market platform offering agents the chance to virtually trade energy within their community [6], seems promising to establish a multi-win situation for the environment, prosumers/consumers, and the utility grid. LEM can empower the community through possible energy cost reduction, which may incentivize additional utilization of local RES as the profit will be kept within the community [7]. There have been several LEM models proposed in the existing literature, and the associated theoretical tools mainly include game theory [8], dynamic pricing [9], and auction [10], etc. In terms of the trading structure, LEM can be categorized as agent-based trading and P2P trading [11,12]. For the agent-based trading [13–15], the trading community may be viewed as a coalition that could gain more profits than any member alone [2]. In [13], an energy sharing model with price-based demand response was proposed for Photovoltaics (PV) prosumers in a microgrid, and a dynamical internal pricing model was formulated based on the PVs' supply and demand ratio (SDR). A cooperative trading model for a community-level energy system was proposed in [14], and a corresponding real-time energy management model was also proposed under cooperative trading considering the prosumers' stochastic characteristics. For peer-to-peer (P2P) models [3,4,16,17], an overview of the P2P markets was provided in [16], including the motivation, challenges, market designs and potential future developments in this field. A distributed electricity trading system to facilitate the P2P electricity sharing amongst prosumers was proposed in [3] based on multi-agent system and blockchain technology. A localized event-driven market mechanism was studied in [4] with the energy trading process built as a Markov decision process, and the role of emerging energy brokers was also explored. In [17], a game-theoretic model for P2P energy trading within a community microgrid was proposed, and [18] gave an overview of the game theory applications in P2P energy trading. There also have been several practical projects being aware of the local trading, such as H2020 EMPOWER project [2] and Brooklyn Microgrid [19].

In the existing studies, we find the mediators, such as aggregator, Smart Energy Service Provider [11], and distributor [20], play important roles in the market design of LEM in terms of simplifying market regulation and the interface with the wholesale market or system operator. Consequently, the community-based trading structures will more likely be actively developed in the near future [21]. In this paper, the trading manager (TM) is involved which can be undertaken by either a third party or the prosumers/consumers, and the TMs can be incentivized by the service fee from other entities. In general, there are multiple TMs coexisting in the LEM, and optimally allocating the entities to multiple TMs (namely the trading community formation) to maximize the overall interests is a challenging problem. [22] and [23] studied the energy trading between microgrids from the perspective of coalitional game with merge-and-split rules applied in the coalition formation. However, this kind of method cannot guarantee the TMs to be distributed in different trading clusters. A more appropriate and effective approach is urgently needed to solve the trading community formation problem, especially in the case with a large number of trading participants.

In addition, the LEMs are mainly performed within a single medium-voltage feeder in most existing studies, and the energy or loads not traded in the LEMs will still participate in the wholesale market. To further facilitate the local trading for entities of different scales, the trading scope can also be expanded to multiple feeders, which may involve high-voltage transmission networks when the trading participants do not belong to the same substation, and the wheeling charge of the transmission networks plays a vital role in the DG trading in some countries [24]. Taking several large-scale entities into account at the same time, the trading network should be established in multiple levels as the trading costs and network constraints may not be the same in each level. How different trading modes could coexist with the existing trading pattern in a multi-level framework needs to be studied accordingly, and how to combine features of the transmission network (e.g., topological structure or wheeling charge) in the LEMs involving multiple feeders is also an open-ended problem. Furthermore, the LEM will have various transaction relation structures when different trading modes are applied. What the characteristics of the trading network will be like with different trading modes and which links are more crucial for the proper operation of the trading network have not been studied yet in the existing research. The complex network (CN) method, which has been used in the power grid [5,25,26], especially in the high voltage networks, is a promising tool to solve these issues in LEM.

Under such a background, this paper proposes a multi-level trading community formation model and the hybrid trading networks are constructed based on the formed communities. The main contributions of this paper are listed as follows:

(1) The trading community formation, which is a mixed integer programming problem, is modeled in a novel way using an Lp-box consensus ADMM algorithm. The network features of physical systems are explicitly represented in the trading community formation model, considering the power loss and wheeling charging at the local trading level and the regional trading level, respectively.

(2) Based on the formed trading communities, hybrid trading networks (namely TA and TPA) are developed with three different trading modes (i.e., traditional trading mode, agent-based trading mode and P2P trading mode), where a new pairing mechanism for P2P trading is established following the principle of rewarding renewable energy generation. All these trading modes can coexist organically within the proposed hybrid trading networks.

(3) Different trading networks including the traditional trading network, TA and TPA trading networks are analyzed based on a set of informative complex network indices. In addition, the link entropy index is applied to evaluate the edge significance in the communication relation network on maintaining global connectivity of the hybrid trading network.

The rest of the paper is organized as follows. The overall framework for trading network formation is presented in Section 2. The distributed optimization for the trading community formation is proposed in Section 3. In Section 4, the process for trading network formation and the communication network for the trading network are presented. In Section 5, a numerical study on a test system with six IEEE 33-bus systems connected through the IEEE 9-bus system is performed to validate the effectiveness of the proposed model and solution method. Finally, conclusions are drawn in Section 6.

2. Framework for trading network formation

In this paper, three types of trading modes are involved in hybrid trading network construction:

- **Traditional trading mode**: all the entities trade with the utility grid based on the trading prices in the wholesale market.
- **Agent-based trading mode**: the entities trade with the TMs, which act as agents or mediators. The TMs here are also in charge of distributing the extra profit generated in LEMs among the entities.
- **P2P trading mode**: the entities can trade with other entities directly. As small-scale electricity consumers and prosumers usually cannot afford a time-consuming search for a particular trading partner [4], in this paper we consider that the P2P tradings would be conducted under the guidance of TMs, and this kind of centralized P2P is also much easier to maintain [27,28].

The trading structures and related information flows for the agent-based and P2P trading modes are illustrated in Fig. 1(a) and (b), respectively. The overall framework for the multi-level hybrid trading network formation is designed as shown in Fig. 2. The traditional trading mode shown in Fig. 2(a) can be regarded as a benchmark scenario. Two trading levels (*i.e.*, the local and regional trading levels) are considered to facilitate the renewable energy consumption. The local trading level mainly focuses on a single medium-voltage feeder while the regional trading level involves multiple feeders (could be within one transformer substation or connected through transmission networks). A general entity in Fig. 2 can be a residential community, a commercial building, a microgrid, a load aggregator, a DG, a storage device, etc. The regional entities consist of the local trading managers and large-scale entities, which are similar with general entities but with significantly larger capacities or outputs, such as a centralized photovoltaic power station, a sizable gas turbine engine.

The TMs enable the entities to take part in the LEM and facilitate different trading modes to coexist with each other. It is assumed that TMs are acted by some of the entities in the grid and will not change in a short period in this study. With the emergence of TMs in each trading level, the trading communities will be formed as shown in Fig. 2(b) based on certain criteria, which will be elaborated in Section 3. For the local trading communities, they consist of multiple entities and are formed within the local trading level, and a feed could consist of one local trading community or multiple ones (we consider multiple ones in the paper for general applicability). For the regional trading communities, they consist of multiple regional entities, which may be located in multiple feeders connected together (within the same transformer substation or not).

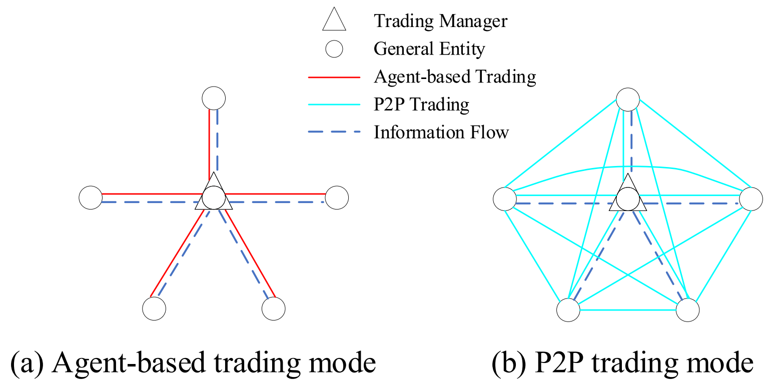

Fig. 1. Structures of the agent-based and P2P trading modes.

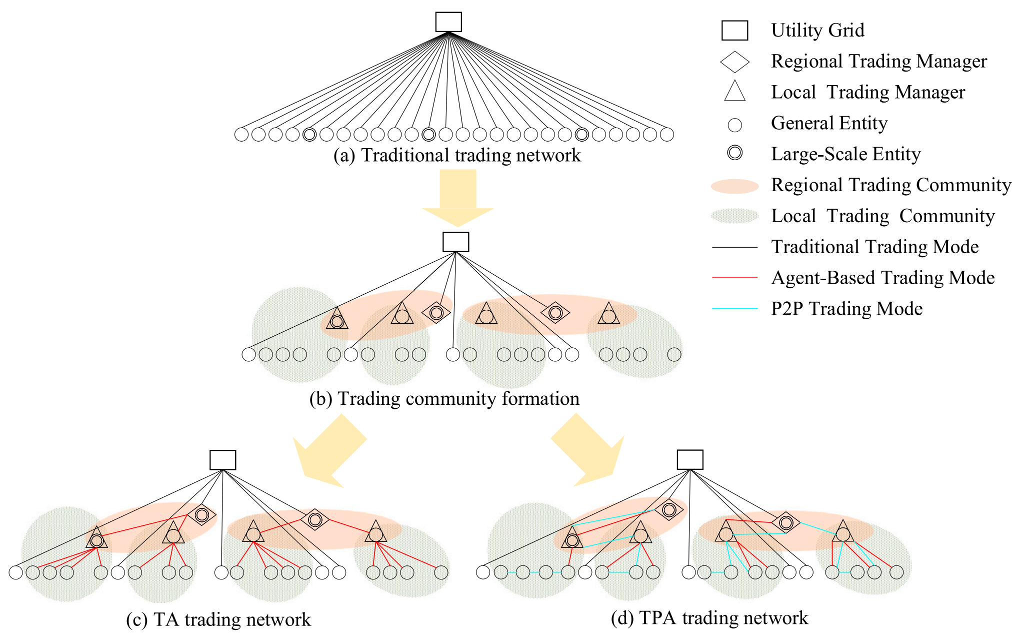

Fig. 2. The framework of multi-level hybrid trading network formation.

When the communities are determined, the hybrid trading networks are formed with the assistance of TMs based on the trading modes of the entities, *i.e.*, the three types of trading modes mentioned previously. Two hybrid trading networks are considered in this paper: the first one includes the traditional trading mode and agent-based trading mode (defined as TA network) while the second one includes the traditional trading mode, P2P trading mode and agent-based trading mode (defined as TPA network):

(1) In the TA hybrid trading network, the entities in the trading community trade with the corresponding TMs at both local and regional trading levels, and the agent-based tradings are represented by red lines in Fig. 2.

(2) In the TPA hybrid trading network, the entities form the P2P trading pairs first (light blue lines in Fig. 2(d)), and the entities with remaining energy/load (not traded in P2P trading) will continue to choose the agent-based mode as shown in Fig. 2(d).

The regional TMs also trade energy with the utility grid in the residual electricity which is not fully traded in the LEM. For those entities not participating in the LEM, they can still apply the traditional trading mode, and it is assumed that all the local TMs will participate in the regional trading in this paper. The black lines in Fig. 2 indicate the trading between entity/TM and the utility grid, and it can be observed that the hybrid trading modes will not conflict with the traditional trading mode. In the following two sections, the trading community formation and the hybrid trading network formation will be presented in detail.

3. Distributed optimization for trading community formation

3.1. Trading community formation based on Lp-box consensus ADMM

As indicated in Fig. 2, the trading community formation for all the entities is important and fundamental in the hybrid trading network formation processes. The TMs are the executor in the trading community formation, while all the entities participating in the LEM will be involved. In this paper, the community formation model aims to maximize the overall interests of the LEM. Taking a system consisting of n_m TMs and n_e entities as an example, the model can be established from a global optimization perspective with the objective $min \sum_{i=1}^{n_m} f_i(\boldsymbol{x})$, where the binary variable vector $\boldsymbol{x} = [x_{11}, \ldots, x_{1n_e}, x_{21}, \ldots, x_{2n_e}, \ldots, x_{n_m1}, \ldots, x_{n_mn_e}]$ indicates the trading community that each entity belongs to, and $\boldsymbol{x}_{jk} = 1$ means the kth entity belongs to the jth community, otherwise $\boldsymbol{x}_{jk} = 0$. In order to protect the privacy of TMs and to address the computational complexity of the centralized approach, the solution of the proposed model could be performed in a distributed manner. In the meantime, the communication reliability can also be guaranteed to some extent as a central coordinator is not needed in a distributed manner. The optimization model can be further transformed into a global consensus problem [29] with separable objectives $\sum_{i=1}^{n_m} f_i(\boldsymbol{x}_i)$ and the constraints $\boldsymbol{x}_i = z, i \in [1, 2, \dots, n_m]$, where z is a common global variable. The global consensus problem can be solved using ADMM, due to its salient performance for online and distributed optimization and its successful applications in a broad range of practical problems. In the community formation model, every single trading community can be regarded as one block in the ADMM approach. However, ADMM is designed for continuous optimization and cannot be adopted directly in the trading community formation problem, which is a mixed integer programming problem. Then the binary constraints in trading community formation are replaced with an equivalent set of continuous constraints, namely the intersection between the box and the (n-1) dimensional sphere [30]. Taking an n-dimensional binary set $\{0,1\}^n$ as an example, it can be equivalently replaced by the intersection between a box and an (n-1)-dimensional sphere (termed the Lp-box intersection) as follows:

$$\boldsymbol{u} \in \{0,1\}^n \Leftrightarrow \boldsymbol{u} \in [0,1]^n \cap \left\{ \boldsymbol{u} : \left\| \boldsymbol{u} - \frac{1}{2}\mathbf{1}_n \right\|_p^p = \frac{n}{2^p} \right\} \tag{1}$$

where the sphere is centered at $\frac{1}{2}\mathbf{1}_n$ with radius $(n^{\frac{1}{p}}/2)$, and $p \in \mathcal{N}$ is a natural number and is set as 2 in this paper.

Then the general model of trading community formation can be represented as follows:

$$\min \quad f(\boldsymbol{x}) = \sum_{i=1}^{n_m} \left[f_i(\boldsymbol{x}_i) + h_i(\boldsymbol{z}_{2i}, \boldsymbol{z}_{3i}) \right] \tag{2}$$

Subject to

$$\boldsymbol{x}_i = \boldsymbol{z}_1 \tag{3}$$

$$\boldsymbol{x}_i = \boldsymbol{z}_{2i}, \quad \boldsymbol{z}_{2i} \in \boldsymbol{S}_b = [\mathbf{0}, \mathbf{1}]^n \tag{4}$$

$$\boldsymbol{x}_i = \boldsymbol{z}_{3i}, \ \boldsymbol{z}_{3i} \in \boldsymbol{S}_p = \left\{ \boldsymbol{z} : \left\| \boldsymbol{z} - \frac{1}{2}\mathbf{1}_n \right\|_2 = \frac{\sqrt{n}}{2} \right\} \tag{5}$$

$$\mathbf{C}\boldsymbol{x}_i = \mathbf{d} \tag{6}$$

where $f_i(\boldsymbol{x}_i)$ is the objective function for community i. $h_i(\boldsymbol{z}_{2i}, \boldsymbol{z}_{3i}) = \mathbb{I}_{\{z_{2i} \in S_b\}} + \mathbb{I}_{\{z_{3i} \in S_p\}}$, and $\mathbb{I}_a$ denotes the indicator function: if a is true, $\mathbb{I}_a = 0$, otherwise $\mathbb{I}_a = \infty$. $\boldsymbol{x}_i = \{\boldsymbol{x}_{ijk}\}_{j \in M, k \in E} = \{x_{i11}, \dots, x_{i1n_e}, x_{i21}, \dots, x_{i2n_e}, \dots, x_{in_m1}, \dots, x_{in_mn_e}\}$ (M is the manager set, $|M| = n_m$; and E is the entity set, $|E| = n_e$). $x_{ijk} = 1$ means the k-th entity will join manager j's community in the variables of manager i, otherwise $x_{ijk} = 0$.

In the above expressions, the constraint (3) is the consensus constraint. The element of $\boldsymbol{x}_i$ should be in the set $\{0,1\}$, which can be expressed as constraints (4) and (5). $\boldsymbol{z}_1$, $\boldsymbol{z}_{2i}$, $\boldsymbol{z}_{3i}$ are corresponding variable vector in these constraints respectively. Constraint (6) represents that each entity can only join one community, and it is a global constraint, $\sum_{j=1}^{n_m} x_{ijk} = 1, k = 1, 2, \dots, n_e$. C and d in Eq. (6) can be represented as:

$$\mathbf{C} = [\underbrace{\mathbf{E}_{n_e}, \mathbf{E}_{n_e}, \dots, \mathbf{E}_{n_e}}_{n_m}], \quad \mathbf{d} = \mathbf{1}_{n_e} \tag{7}$$

The augmented Lagrangian form of the above optimization problem can be expressed as follows:

$$L_\rho(\boldsymbol{x}, \boldsymbol{y}, \boldsymbol{z}) = \sum_{i=1}^{n_m} L_{\rho i}(\boldsymbol{x}, \boldsymbol{y}, \boldsymbol{z}) \tag{8}$$

$$\begin{aligned} L_{\rho i}(\boldsymbol{x}, \boldsymbol{y}, \boldsymbol{z}) = \sum_{i=1}^{n_m} \Big[& f_i(\boldsymbol{x}_i) + h_i(\boldsymbol{z}_{2i}, \boldsymbol{z}_{3i}) \\ & + \boldsymbol{y}_{1i}^T(\boldsymbol{x}_i - \boldsymbol{z}_1) + \frac{\rho_1}{2}\|\boldsymbol{x}_i - \boldsymbol{z}_1\|_2^2 \\ & + \boldsymbol{y}_{2i}^T(\boldsymbol{x}_i - \boldsymbol{z}_{2i}) + \frac{\rho_2}{2}\|\boldsymbol{x}_i - \boldsymbol{z}_{2i}\|_2^2 \\ & + \boldsymbol{y}_{3i}^T(\boldsymbol{x}_i - \boldsymbol{z}_{3i}) + \frac{\rho_3}{2}\|\boldsymbol{x}_i - \boldsymbol{z}_{3i}\|_2^2 \\ & + \boldsymbol{y}_{4i}^T(\mathbf{C}\boldsymbol{x}_i - \mathbf{d}) + \frac{\rho_4}{2}\|\mathbf{C}\boldsymbol{x}_i - \mathbf{d}\|_2^2 \Big] \end{aligned} \tag{9}$$

The ADMM update steps are performed based on the above augmented Lagrangian format, and the update steps at the kth iteration are as follows:

$$\boldsymbol{x}_i^{k+1} = \underset{\boldsymbol{x}_i}{\mathbf{argmin}} L_{\rho i}(\boldsymbol{x}, \boldsymbol{y}^k, \boldsymbol{z}^k) \tag{10}$$

$$\boldsymbol{z}_1^{k+1} = \frac{1}{n_m} \sum_{i=1}^{n_m} \left(\boldsymbol{x}_i^{k+1} + \frac{1}{\rho_1}\boldsymbol{y}_{1i}^k \right) \tag{11}$$

$$\boldsymbol{z}_{2i}^{k+1} = \underset{z_{2i} \in S_b}{\mathbf{argmin}} \ \boldsymbol{y}_{2i}^{kT}(\boldsymbol{x}_i^{k+1} - \boldsymbol{z}_{2i}) + \frac{\rho_2}{2}\left\|\boldsymbol{x}_i^{k+1} - \boldsymbol{z}_{2i}\right\|_2^2 \tag{12}$$

$$\boldsymbol{z}_{3i}^{k+1} = \underset{z_{3i} \in S_p}{\mathbf{argmin}} \ \boldsymbol{y}_{3i}^{kT}(\boldsymbol{x}_i^{k+1} - \boldsymbol{z}_{3i}) + \frac{\rho_3}{2}\left\|\boldsymbol{x}_i^{k+1} - \boldsymbol{z}_{3i}\right\|_2^2 \tag{13}$$

$$\boldsymbol{y}_{1i}^{k+1} = \boldsymbol{y}_{1i}^k + \rho_1(\boldsymbol{x}_i^{k+1} - \boldsymbol{z}_1^{k+1}) \tag{14}$$

$$\boldsymbol{y}_{2i}^{k+1} = \boldsymbol{y}_{2i}^k + \rho_2(\boldsymbol{x}_i^{k+1} - \boldsymbol{z}_{2i}^{k+1}) \tag{15}$$

$$\boldsymbol{y}_{3i}^{k+1} = \boldsymbol{y}_{3i}^k + \rho_3(\boldsymbol{x}_i^{k+1} - \boldsymbol{z}_{3i}^{k+1}) \tag{16}$$

$$\boldsymbol{y}_{4i}^{k+1} = \boldsymbol{y}_{4i}^k + \rho_4(\mathbf{C}\boldsymbol{x}_i^{k+1} - \mathbf{d}) \tag{17}$$

The update of $\boldsymbol{z}_{2i}^{k+1}$ and $\boldsymbol{z}_{3i}^{k+1}$ can also be calculated based on the projection operators $\mathbf{P}_{S_b}$ and $\mathbf{P}_{S_p}$ directly as follows [30]:

$$\begin{aligned} & \boldsymbol{z}_{2i}^{k+1} = \mathbf{P}_{S_b}\left(\boldsymbol{x}_i^{k+1} + \frac{1}{\rho_2}\boldsymbol{y}_{2i}^k \right), \\ & \mathbf{P}_{S_b}(\boldsymbol{a}) = min(\mathbf{1}_n, max(\mathbf{0}_n, \boldsymbol{a})) \end{aligned} \tag{18}$$

$$\begin{aligned} & \boldsymbol{z}_{3i}^{k+1} = \mathbf{P}_{S_p}\left(\boldsymbol{x}_i^{k+1} + \frac{1}{\rho_3}\boldsymbol{y}_{3i}^k \right), \\ & \mathbf{P}_{S_p}(\boldsymbol{a}) = \frac{\sqrt{n}}{2}\frac{\overline{\boldsymbol{a}}}{\|\overline{\boldsymbol{a}}\|_2} + \frac{1}{2}\mathbf{1}_n, \overline{\boldsymbol{a}} = \boldsymbol{a} - \frac{1}{2}\mathbf{1}_n \end{aligned} \tag{19}$$

In the proposed ADMM model, all the involved variables can be updated locally in each block, and only the update of z_1 needs to collect the information of $\boldsymbol{x}$ and $\boldsymbol{y}$ from all the blocks. The convergence proof of the proposed ADMM model is presented in Appendix A.

3.2. Optimization objectives for each trading level

As the trading costs and network constraints may not be the same at different trading levels, we construct the objective functions for the local and regional trading levels respectively. The trading community formation at the local level is realized within each feeder, while the trading community formation at the regional level involves several feeders.

(1) At the local trading level, the objective of the community formation is to maximize the profit increase subtracting the simulated power loss in the trading:

$$\min f(\boldsymbol{x}) = \sum_{i=1}^{n_{mf}} f_i(\boldsymbol{x}_i) = \sum_{i=1}^{n_{mf}} -\left(\Delta C_i^t - P_{loss\_i}^t \right) \tag{20}$$

$$\Delta C_i^t = (p_s^t - p_b^t) V_i^t \tag{21}$$

$$V_i^t = min\left[\sum_{k=1}^{n_{ef}} max(P_{ik}^t, 0), -\sum_{k=1}^{n_{ef}} min(P_{ik}^t, 0) \right] \tag{22}$$

$$P_{ik}^t = x_{iik} P_k^t \tag{23}$$

$$P_{loss\_i}^t = p_s^t \sum_{k=1}^{n_{ef}} \left(\left| P_{ik}^t \right| r_{loss} \rho \frac{d_{ik}}{d_{ave}} \right) \tag{24}$$

(2) At the regional trading level, the trading community formation is performed based on the community formation results of the local trading level, where the output/load of each local community is determined. The objective of the community formation is to maximize the profit increase subtracting the wheeling charge of the transmission network incurred in the trading:

$$\min f(\boldsymbol{x}) = \sum_{p=1}^{N_M} f_p(\boldsymbol{x}_p) = \sum_{p=1}^{N_M} -\left(\Delta C_p^t - C_{whp}^t \right) \tag{25}$$

$$\Delta C_p^t = \left(p_s^t - p_b^t\right) V_p^t \tag{26}$$

$$V_p^t = min\left[\sum_{q=1}^{N_E} max\left(P_{pq}^t, 0\right), -\sum_{q=1}^{N_E} min\left(P_{pq}^t, 0\right)\right] \tag{27}$$

$$P_{pq}^t = x_{ppq} P_q^t \tag{28}$$

$$C_{whp}^t = p_{wh}^t \sum_{l=1}^{n_l} \left| \boldsymbol{PTDF}_l \left(\boldsymbol{Pin}_{p1}^t + \cdots + \boldsymbol{Pin}_{pN_E}^t\right)\right| \tag{29}$$

where $\boldsymbol{Pin}_{pq}^t$ is the power injection vector (column vector) of all nodes in the transmission network, reflecting the trade between regional TM p and regional entity q (the pth element in $\boldsymbol{Pin}_{pq}^t$ is P_{pq}^t, and the qth element is $-P_{pq}^t$); and $\boldsymbol{PTDF}_l$ is the lth row in the power transfer distribution factor (PTDF) matrix [31], which is represented in Eq. (30).

$$\boldsymbol{PTDF} = \boldsymbol{H}'(\boldsymbol{B}')^{-1} \tag{30}$$

where $\boldsymbol{H}'$ and $\boldsymbol{B}'$ are sub-matrices, obtained respectively from the admittance matrix $\boldsymbol{B}$ and transmission matrix $\boldsymbol{H}$ by deleting the row and column (only the column in case of $\boldsymbol{H}$) corresponding to the slack node; and X_{ij} is the reactance of the line with end nodes i and j.

$$\boldsymbol{B}_{ii} = \sum_{j \neq i} \frac{1}{X_{ij}}; \boldsymbol{B}_{ij} = -\frac{1}{X_{ij}},\ i \neq j; \tag{31}$$

$$\boldsymbol{H}_{li} = -\boldsymbol{H}_{lj} = \frac{1}{X_{ij}};\ \boldsymbol{H}_{lk} = 0 \quad \forall k \neq i, j \tag{32}$$

4. Trading network formation and analysis

As shown in Fig. 2, based on the trading community formation results, more specific trading relationships between entities (including the TMs) in each trading community need to be determined. We name this process as trading network formation, which is performed according to the trading mode, *i.e.*, TA and TPA, and it is also closely related to the profit allocation within the trading communities. In this paper, the trading community formation and hybrid trading network construction are developed based on the prespecified load/generation information of the entities. To guarantee that the nodal voltages and line currents are kept within a reasonable range, the power flow calculation could be conducted in advance, and the nodal load/generation can be adjusted if the constraints are not satisfied. The power flow calculation could be performed based on the Newton–Raphson model [32] or DistFlow method [33]. The former is applicable to both transmission and distribution systems, and the latter is only applicable to distribution systems. The detailed power flow models are introduced in Appendix B.

4.1. Trading network formation and profit allocation with TA trading mode

(1) Network formation in the TA mode

From the red lines shown in Fig. 2(c), the entities in the generated trading communities are all connected to the corresponding TMs in the same communities in the TA mode.

(2) Profit allocation in the TA mode

Within a specified local/regional trading community, the generated profit can be determined based on the optimization objective in Eq. (25)/(20), for example, $-f_p\left(\boldsymbol{x}_p\right)$ and $-f_i\left(\boldsymbol{x}_i\right)$ are the profits of the pth regional trading community and the ith local trading community respectively. After deducting a certain service charging proportion from the profit for the TM, the residual profit is equally distributed between the selling entities and buying entities as both groups contribute to the profit increase in the trading community. For each entity, its profit increase (compared with the traditional trading networks) is related to its power output/load proportion in the total power output/load of the community. In addition, as the local TM also participates in the regional trading, it should further allocate the profit obtained in the regional level to the entities (in the same community with this TM) who make contributions in the regional trading, and generally only one group in selling entities and buying entities can divide this extra profit according to their output/load proportions. More detailed profit allocation for the TA network can be found in Appendix C.

4.2. Trading network formation and profit allocation with TPA trading mode

(1) Network formation in the TPA mode

As mentioned in Section 2, the entities form P2P trading pairs first in the TPA mode. Forming P2P trading pairs also means determining the trading partners and volumes between the buying entities and selling entities. As a vital component in the P2P market mechanism, the trading pairing problem has been studied in some existing research [12,16,34]. Different from the existing rules, a new pairing mechanism for P2P trading is established in this paper, following the principle of rewarding renewable energy generation to better facilitate the utilization of RES. Under this trading pairing rule, the entity with a larger renewable energy output (REO) will be given a higher priority to choose the trading partners, and the trading distance is an important factor in choosing partners [12,16]. The detailed realization process of the proposed P2P pairing mechanism is shown in Fig. 3.

It is assumed that all the entities in the community have been divided into the selling entities and the buying entities before performing the P2P pairing. The selling entities are sorted by their power outputs in a descending order at the beginning of the process. Then the entity with the largest power output (i=1) chooses its nearest buying entity as the trading partner, and the trading volume can be set as the minimum value between the selling entity's power output and the buying entity's demand (this minimum value is also called the maximum possible trading volume as shown in Fig. 3). After performing each pairing operation, the selling entity's power output and the buying entity's demand should be updated, *i.e.*, the traded energy and demand should be subtracted from the corresponding entities' power output/demand. If the selling entity's power output is not sold out with the nearest buying entity, it continues to trade with the other nearest buying entities until its remaining energy is sold out. Next, the selling entity with the second largest power output will perform the similar procedure, and the process will be repeated for the remaining selling entities. The P2P pairing process continues until all the energy is sold out or all the demands are satisfied.

After performing the P2P trading pairing, the entities with residual power outputs/demands will continue to choose the agent-based energy trading mode, and the trading network formation for this part is similar to the TA mode. The trading network with the TPA mode is shown in Fig. 2(d), where the blue lines show the P2P tradings between entities while the red lines still indicate the agent-based tradings.

(2) Profit allocation in the TPA mode

The generated profit of a community in the TPA mode is the same as that in the TA mode, and it is also equally distributed between selling entities and buying entities. The difference is that the profit will be allocated to each entity according to the P2P trading volume proportion rather than the power demand/power output proportion in the agent-based trading. This means an entity who participates in the P2P trading with more power demand/power output will get more profit. Similarly, the local TM will further allocate the profit obtained in regional trading to the related entities who make contributions according to their residual power demands/power outputs(the electricity not traded in the local P2P tradings). More detailed profit allocation for the TPA network can be found in Appendix D.

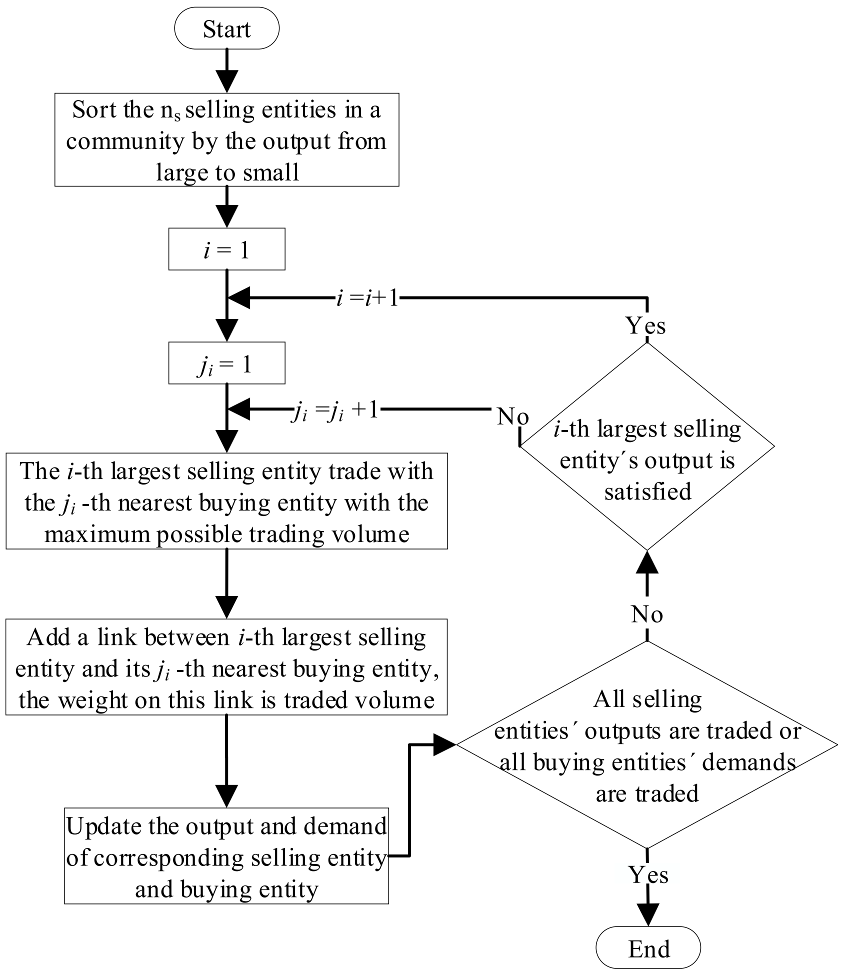

Fig. 3. Realization process of the P2P pairing mechanism.

4.3. Communication network in LEM

The implementation of LEMs has a strong dependence on the information and communication technology (ICT) [35], and the advanced two-way communication networks are expected to be more widely integrated to provide necessary facilities for the LEMs. As implementing private ICT infrastructures for LEMs is not cost-effective, some existing communication networks can be utilized in the LEM, such as the widely used wired broadband network [36]. According to the distributed optimization models, the community formation process depends on the communication between the entities and TMs. Fig. 4 shows the communication network for the hybrid trading network in this paper, and it is applicable to both TA and TPA networks. Within the same feeder, all the entities need to connect with all the local trading managers [37], and the trading managers will also connect with each other. As shown in Fig. 4, the second local TM and the third local TM are within the same feeder, and they are connected with each other. At the regional trading level, all the regional entities are connected with the regional TMs, as indicated by the brown lines in the figure.

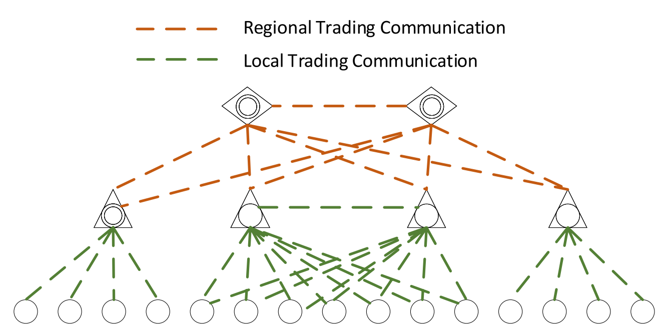

Fig. 4. The communication relation network for the hybrid trading.

4.4. Analysis of trading networks and its communication network

In this paper, the LEM has various transaction relation structures when different trading modes are applied, and the characteristics of the trading network with different trading modes have not been covered yet in the existing literature. The complex network (CN) method, which has been widely used in the power grid [5,25,26], is a useful tool to reflect the network characteristics in LEM. To analyze the network characteristics of different trading networks, some CN indices are adopted in this paper, and the calculation methods for these indices are described in Appendix E.

In addition, it is also important to quantify the impacts of communication system performance on the operations of the LEMs as it will create another level of uncertainty, and trading entities may make suboptimal choices due to the loss of communications [38]. In this paper, the edge importance in the communication network is evaluated using the index of link entropy (LE), which is described in Appendix F.

Table 1
Basic information of each distribution feeder.

Feeder	Manager amount	Total net load	Feeder	Manager amount	Total net load
D1	3	−1755 kw	D4	4	−1398 kw
D2	5	636 kw	D5	3	1316 kw
D3	4	1249 kw	D6	5	−1599 kw

Table 2
Entity distribution between each TM.

Trading level	Community number				
	1	2	3	4	5
Feeder D1 (Local)	11	9	13	–	–
Feeder D5 (Local)	11	9	13	–	–
Feeder D4 (Local)	19	8	3	3	–
Feeder D3 (Local)	11	15	6	1	–
Feeder D6 (Local)	17	6	5	1	4
Feeder D2 (Local)	15	1	15	1	1
Regional	11	15	–	–	–

5. Case study

5.1. Basic data

The proposed models are validated on a test system consisting of an IEEE 9-bus transmission network and six IEEE 33-bus distribution networks, as shown in Fig. 5. It is assumed that only one feeder (corresponding to an IEEE 33-bus network) in each transmission network node will take part in the hybrid trading network. Two regional trading managers are designated in the case, which are the large consumer connected to node 7 (3250 kW) and the large DG connected to node 6 (−2500 kW). There are total 24 local trading managers. The parameters of each feeder are shown in Table 1. The selling and buying prices of the wholesale market (p_s^t and p_b^t) are set as \$0.184 and \$0.092, respectively.

5.2. Community formation results

The community formation for each feeder and the whole regional trading level are performed based on Eqs. (2)–(6). The communities' profit iterations for all feeders are shown in Fig. 6. Each trading community formation process converges within 50 iterations, and the computational time is less than 30 s using Gurobi in Yalmip toolbox under the Matlab environment on a personal computer with Intel Core i5-8300H CPU @ 2.3-GHz and 16GB-RAM. The numbers of entities distributed in each trading community are shown in Table 2.

According to Table 2, the entities are unevenly distributed to the TMs in the trading communities. For feeders D2, D3 and D6 in the local trading level, some TMs do not attract other entities to take part in the communities except for themselves (corresponding to the number "1" in the table), which means not all the TMs can get extra profit in the hybrid trading network as the community formation process is greatly related to load characteristics of the TMs and the surrounding entities.

5.3. Profit increase allocation results

The profit increases of all the entities in the traditional trading network, which is a benchmark for the two hybrid trading networks, are all equal to zero. The profit increase allocation results with the TA and TPA trading networks are shown in Table 3. It can be observed that all the local/regional entities will get benefits in the TA trading network, while only part of the entities will profit from the TPA trading network. We also analyze the correlation between the profit increases and absolute loads of the benefited entities in the TA and TPA networks respectively, and the correlation coefficient between them in the TA network is 0.716 while the value is 0.834 in the TPA network. It means that the values of the power output/load will have greater influence on the profit increases in the TPA network compared with the case in the TA network.

Table 3
Profit increase allocation results.

Trading network type	Number of benefited local entities	Average profit increase of local entities	Number of benefited regional entities	Average profit increase of regional entities
TA network	198	\$3.82	26	\$18.26
TPA network	131	\$6.11	5	\$94.95

5.4. Comparison between different trading strategies

In this subsection, we will mainly compare the profit allocation method used in this paper with some existing local trading mechanisms. Without loss of generality, the comparisons will be performed only at the local trading level involving 198 entities on 6 feeders, as most existing studies mainly consider just one trading level. The comparisons for the agent-based trading and P2P trading are considered separately in the next section.

(1) Agent-based trading

For the agent-based trading, several trading mechanisms were adopted in the existing studies, such as SDR [13], mid-market rate (MMR) [39], and contribution-based method from a perspective of coalitional game [14], etc. These three methods are utilized in the local agent-based trading in the test system as shown in Fig. 5. For a fairer comparison, the power loss and service charging of TMs are also considered in each of these methods: firstly, the profit increase of each entity is calculated using these methods without considering power loss and service charging of TM, respectively; then the total profit increase in a trading community considering the power loss and service charging of TM are allocated to each entity in proportion to the profit increases obtained without considering the power loss and service charging of TM.

According to the calculation results, the profit increase of each entity using the proposed method is the same as that using MMR. The calculation processes of these two methods are different as the latter needs to determine the trading prices first and then calculate the profit increase, while the proposed method does not need to determine the trading prices and the power loss and service charging can also be more easily integrated in the profit calculation process. To make the comparison between these methods clearer, the final equivalent trading prices are calculated for all the entities, and the results are shown in Fig. 7. The wholesale buying price in Fig. 7 is the same as p_s^t, while the wholesale selling price is the same as p_b^t. The vertical dotted line in Fig. 7 is used to divide the sellers (the left side of the line) and the buyers (the right side of the line). The sellers' average selling prices, buyers' buying prices and the number of benefited entities with different agent-based trading strategies are listed in Table 4. For a small number of entities, the contribution-based method brings about higher selling prices and lower buying prices, while its number of benefited entities (47) is less than the results obtained using the other two methods. For the SDR method, its average selling price and average buying price are both the lowest among the three methods, and 109 entities get benefits. In the method used in this paper, all entities can benefit from the local trading, and the average selling price is the highest among the three methods, while the average buying price is higher than SDR but is the same as the contribution-based method.

(2) P2P trading

In this section, the proposed REO-first P2P pairing mode is compared with an existing distance-first pairing mode [12,16]. In the distance-first pairing mode, the P2P trading is performed according to

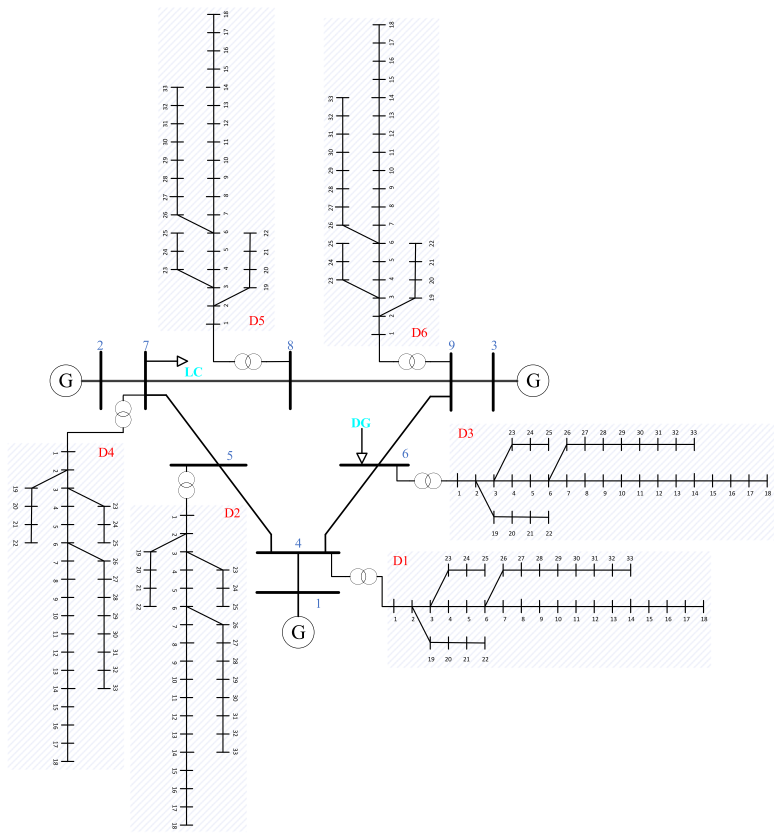

Fig. 5. A test system with IEEE 9-bus and 33-bus networks.

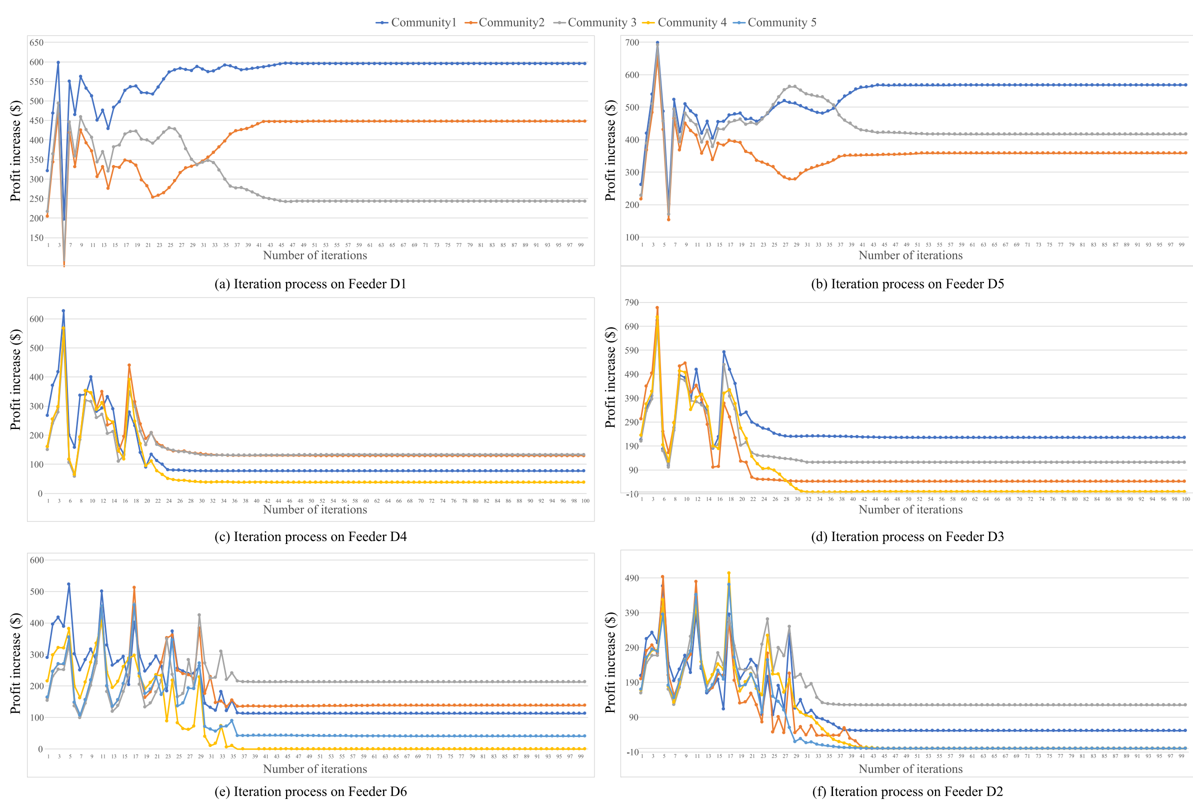

Fig. 6. Iterative process of profit increase in local trading community formation for all feeders.

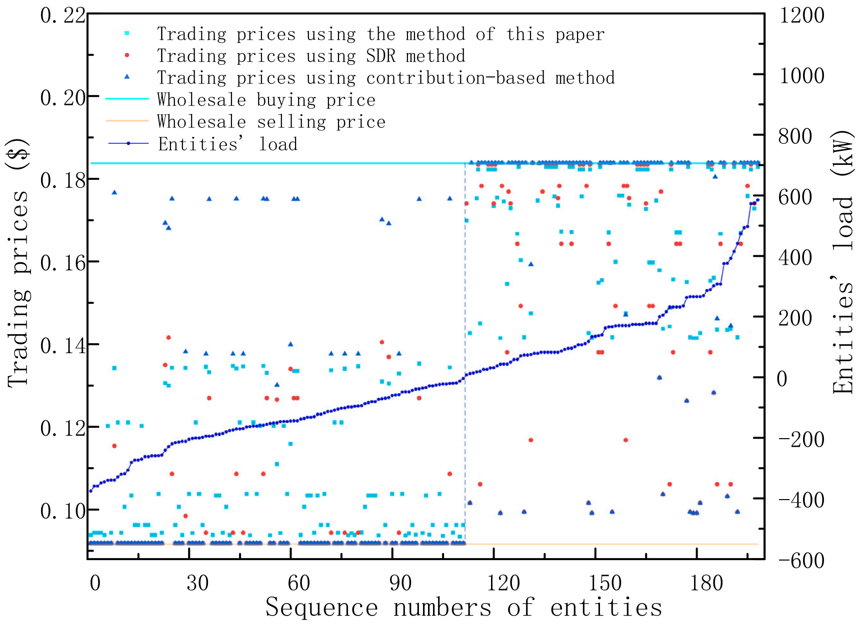

Fig. 7. Trading prices of different strategies for agent-based local trading.

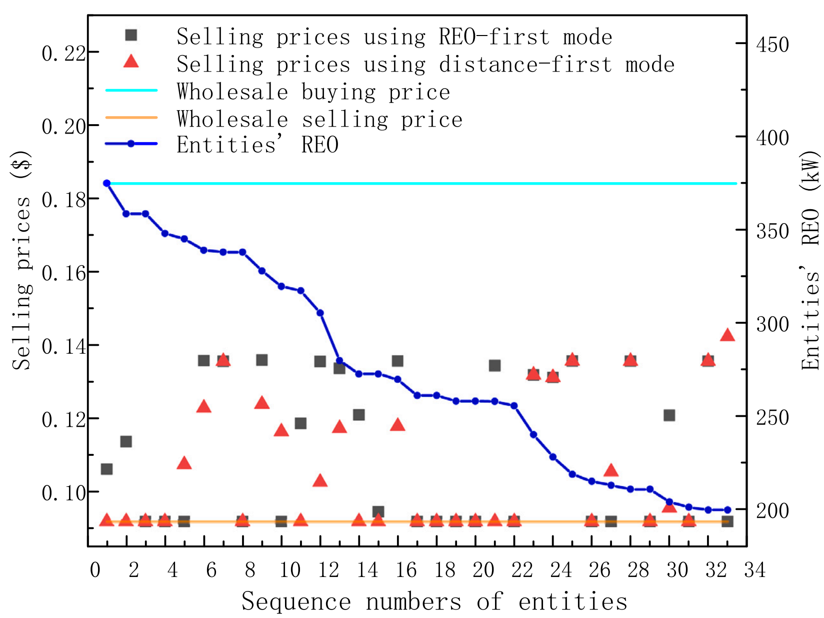

Fig. 8. Comparison between different strategies for the P2P local trading.

Table 4
Average trading prices and the number of benefited entities with different strategies.

Strategies	Sellers' average price ($)	Buyers' average price ($)	Number of benefited entities
SDR	0.097	0.157	109
Contribution-based	0.106	0.167	47
This paper	0.107	0.167	198

the distance between the buying entity and the selling entity, which means the trading with the shortest distance will be performed firstly, followed by the one with the second shortest distance, and so on. In order to make these two modes comparable, other associated settings are all the same except that the P2P trading sequences between the buying entities and selling entities are different, and the trading volumes will also be affected by the P2P trading sequences. The selling price results in local-level trading using the two modes are shown in Fig. 8, and only the top 30% sellers with the largest REO are involved in the figure to show the comparison more clearly. For the 33 selling entities involved in Fig. 8, the numbers of benefited entities are 15 and 18 within the distance-first mode and the REO-first mode, respectively, while selling prices of the latter outperform those of the distance-first mode. The results show that the REO-first mode in P2P pairing is more stimulating for the selling entities with larger REOs, which is instrumental in facilitating the partition of renewable energy resources in the local energy market.

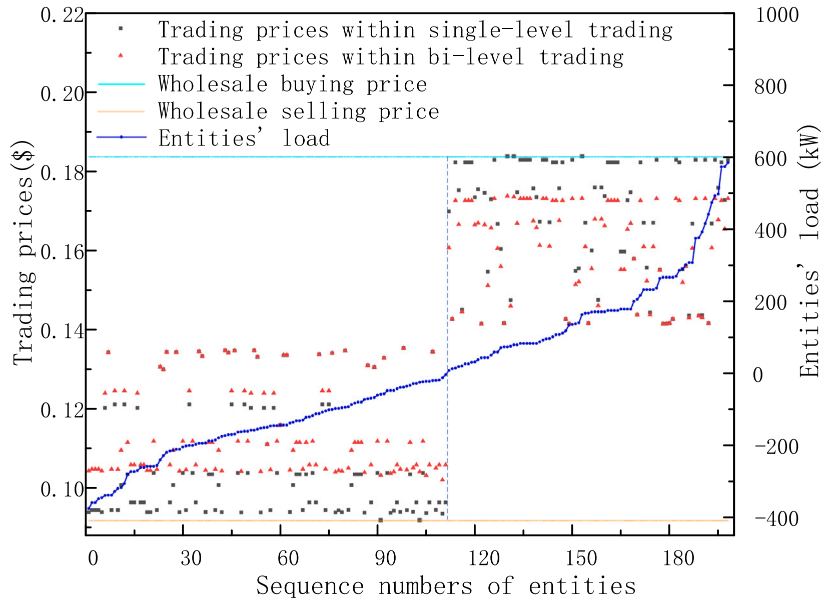

Fig. 9. Comparison between single-level and bi-level agent-based local trading.

Table 5
Average trading prices and the number of benefited entities for single-level trading and bi-level trading.

Strategies	Sellers' average price ($)	Buyers' average price ($)	Number of benefited entities
Single-level agent-based	0.107	0.167	198
Bi-level agent-based	0.114	0.161	198
Single-level P2P	0.108	0.164	99
Bi-level P2P	0.116	0.159	139

Table 6
Indices calculation results.

Network type	AD	AWD	Modularity	APL	ACC	Density
Traditional	1.05	54.36	0.00	1.98	0	0.005
TA	1.12	71.08	0.47	5.38	0.024	0.006
TPA	1.05	58.36	0.45	5.37	0.015	0.005

5.5. Comparison between single-level trading and bi-level trading

In this section, the bi-level trading will be compared with the extensively studied single-level trading for both agent-based trading and P2P trading. The comparative result for agent-based trading is shown in Fig. 9, and the regional trading level further benefits 158 local entities, which means their trading prices are better than those who just participate in single-level trading. For the P2P trading, the comparison result is shown in Fig. 10, and the numbers of benefited entities in single-level and bi-level P2P trading are 99 and 139, respectively. According to Figs. 9, 10 and Table 5, the entities' prices in bi-level trading are significantly improved compared with those in single-level trading both for agent-based trading and P2P trading.

5.6. Network characteristics analysis for different trading networks

(1) Trading network analysis

Fig. 11 shows three trading networks with different trading modes, *i.e.*, the traditional trading, TA trading and TPA trading. The biggest black spot represents the utility grid, and the smallest ones represent the general entities. The regional and local TMs are marked as the black spots with the sizes between the above mentioned two types. The complex network indices' calculation results are shown in Table 6. Among these indices, AD, ACC and Density mainly reflect the edge intensity of the network; Modularity reflects how good the community structures are in the network; APL reflects the overall average distance of all possible node pairs in the network. For the AD index and density, the values with the TA trading network are a little higher than the values in the traditional and TPA networks. For AWD, the value in TA is also apparently higher than the values in the other two networks. The modularity and APL values in TA and TPA are very close and much higher than the corresponding values in the traditional network. The ACC value in TA is a bit higher than that in TPA, while the traditional one is zero. The densities in these three trading networks are very close.

(2) Communication network analysis

The LE index mainly represents the edge significance on maintaining the global connectivity in a network. The LE calculation based on Section 4-B for the whole communication network are shown in Fig. 12. In Fig. 12, the two black spots in the middle represent the regional TMs, and the bigger black spots in the surrounding represent the local TMs while the smaller ones represent the general entities. It can be seen that the connections between the local managers and regional managers have larger LE values, among which the values of the feeders with three local managers are the largest. For the links between the local entities and local managers, a feeder with fewer managers is likely to have larger LE values. The connections with larger LE values are more important in maintaining the hybrid trading network's connectivity.

6. Conclusions

It is practical and pressing to establish a more flexible market scheme with which localized energy trading could be promoted. This paper proposes a multi-level trading community formation model and the constructing procedures for corresponding hybrid trading networks. To properly allocate the entities among multiple trading managers,

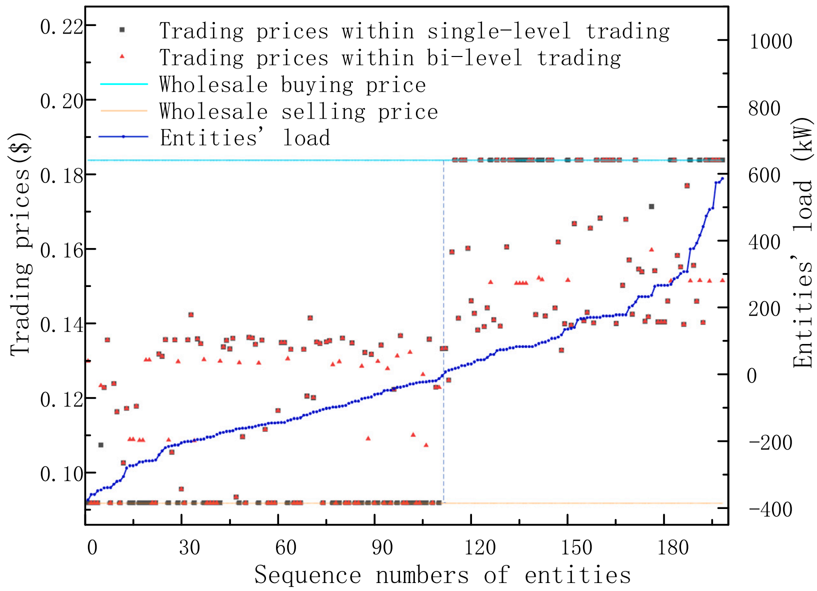

Fig. 10. Comparison between single-level and bi-level P2P local trading.

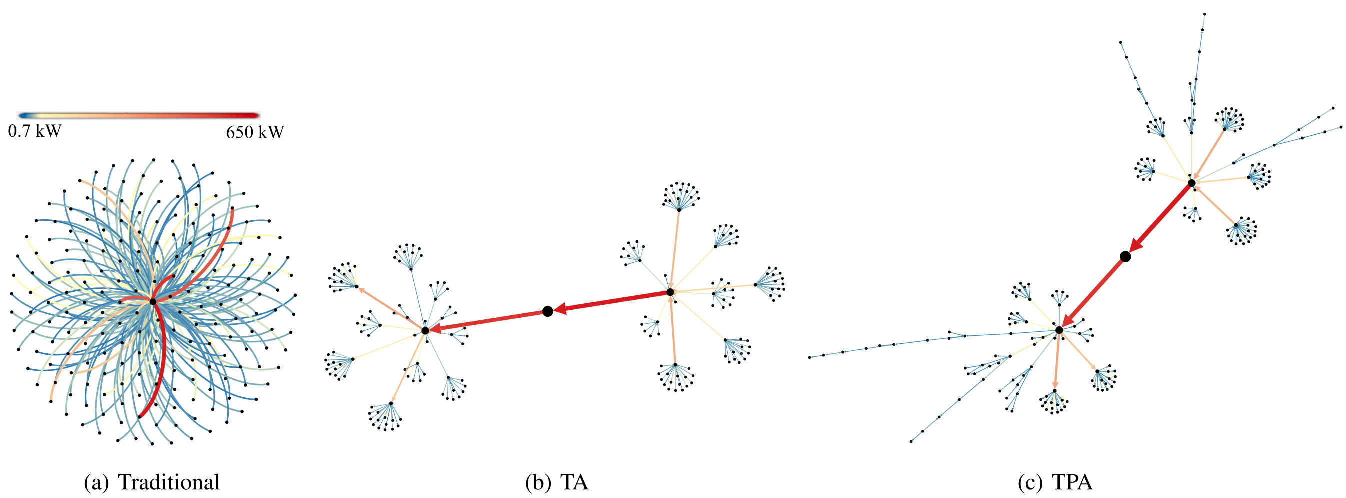

Fig. 11. Trading networks in different trading modes.

the optimization model for the trading community formation is proposed based on the Lp-box consensus alternating direction method of multipliers (ADMM), and corresponding objective functions are defined for the local trading level and regional trading level respectively considering the network features. The proposed community formation model can be adapted to large-scale trading participants efficiently in a distributed way. Based on the three trading modes (*i.e.*, the traditional trading mode, agent-based trading mode and peer-to-peer (P2P) trading mode), two hybrid trading networks are developed——the hybrid trading network integrating the traditional trading mode and agent-based trading mode (defined as TA network), and the hybrid trading network integrating the traditional trading mode, P2P and agent-based trading modes (defined as TPA network). For the P2P pairing process, a new mechanism following the principle of rewarding renewable energy generation is established. The corresponding profit allocation methods are presented for TA and TPA trading networks respectively considering the service fees for the trading managers (TMs). A set of complex network indices is introduced in the paper and applied to analyze the network characteristics of different trading networks. In order to explore the important edges in the trading networks, the link entropy (LE) index is adopted to evaluate the edge significance in communication networks on maintaining the global connectivity of the hybrid trading networks. Finally, via a test system with an IEEE 9-bus transmission system and six IEEE 33-bus systems, the validity of the proposed models is confirmed. Different trading strategies are compared for the agent-based and the P2P trading: the agent-based strategy used in this paper can benefit all entities compared with the supply and demand ratio and contribution-based strategies, while the renewable energy output (REO)-first mode proposed for P2P pairing is more stimulating for the selling entities with larger renewable energy outputs than the distance-first mode. In addition, the bi-level trading is compared with the widely-used single-level local trading, indicating that the entities' prices in the bi-level trading are significantly improved compared with those of the single-level trading both for agent-based trading and P2P trading. The proposed models for trading community formation and trading network formation are instrumental in developing sustainable local energy markets. In the future work, the optimization model on the demand side (e.g., demand response and energy storage systems) could be investigated to further facilitate the local consumption of renewable energy resources.

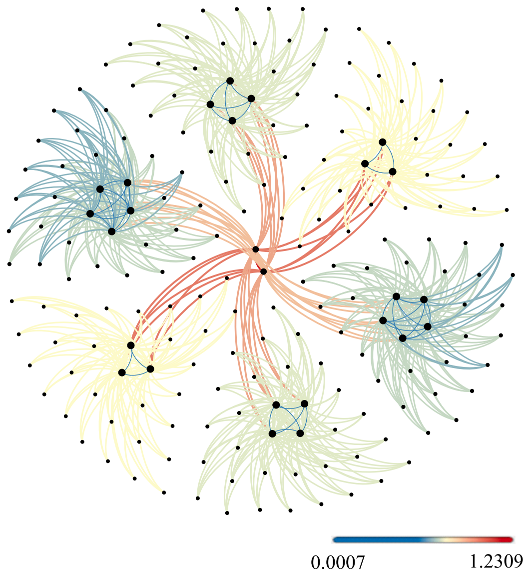

Fig. 12. LE evaluation results for communication network.

CRediT authorship contribution statement

Li Ma: Conceptualization, Methodology, Software, Validation, Formal analysis, Investigation, Data curation, Writing - original draft, Visualization. **Lingfeng Wang:** Conceptualization, Methodology, Resources, Writing - review & editing, Supervision, Project administration, Funding acquisition. **Zhaoxi Liu:** Conceptualization, Writing - review & editing.

Declaration of competing interest

The authors declare that they have no known competing financial interests or personal relationships that could have appeared to influence the work reported in this paper.

Acknowledgment

This work was supported in part by the U.S. National Science Foundation Industry/University Cooperative Research Center on Grid-connected Advanced Power Electronic Systems (GRAPES) under Award GR-17-14.

Appendix A. Convergence proof of the proposed ADMM model

Here the convergence of the Lp-box consensus ADMM model in the local trading level will be proved, that means the $f_i(\boldsymbol{x}_i)$ in expression (9) is the same with that in expression (20). For the expression (20), it can further be transformed to the following expression:

$$\min f(\boldsymbol{x}) = \sum_{i=1}^{n_{mf}} f_i(\boldsymbol{x}_i) = \sum_{i=1}^{n_{mf}} -\left(\Delta C_i^t - P_{loss\_i}^t\right) \tag{33}$$

$$\Delta C_i^t = \left(p_s^t - p_b^t\right)\sum_{k=1}^{n_{ef}}\left(a_{ik}P_{ik}^t\right) \tag{34}$$

$$P_{loss\_i}^t = p_s^t \sum_{k=1}^{n_{ef}}\left(b_{ik}P_{ik}^t r_{loss}\rho\frac{d_{ik}}{d_{ave}}\right) \tag{35}$$

$$P_{ik}^t = x_{iik}P_k^t \tag{36}$$

$$a_{ik} = \begin{cases} 0, & \alpha_i > \beta_i, P_{ik}^t \geqslant 0 \\ & \text{or } \alpha_i < \beta_i, P_{ik}^t < 0 \\ 1, & \alpha_i \leqslant \beta_i, P_{ik}^t \geqslant 0 \\ -1, & \alpha_i > \beta_i, P_{ik}^t < 0 \end{cases} \tag{37}$$

$$\alpha_i = \sum_{k=1}^{n_{ef}} max\left(P_{ik}^t, 0\right), \beta_i = -\sum_{k=1}^{n_{ef}} min\left(P_{ik}^t, 0\right) \tag{38}$$

$$b_{ik} = \begin{cases} 1, & P_{ik}^t \geqslant 0 \\ -1, & P_{ik}^t < 0 \end{cases} \tag{39}$$

Notice that $f_i(\boldsymbol{x}_i)$ in the above expressions are linear piecewise functions, as defined in Definition **1** in [40]. According to [40], the convergence conditions for ADMM with $f_i(\boldsymbol{x}_i)$ being linear piecewise function are as follows:

(1) $f(\boldsymbol{x})$ in expression (2) is coercive over the feasible set $(\boldsymbol{x}, \boldsymbol{z})$, and the details are similar with the assumption A1 in [40].

(2) $h_i(z_{2i}, z_{3i})$ is Lipschitz differentiable. According to the definition of $h_i(\cdot)$, it is equal to 0 when $z_{2i\in S_b}$ and $z_{3i\in S_p}$, and a constant function is Lipschitz differentiable.

(3) Representing the constraints as $C'\mathbf{x} + D\mathbf{z} = \mathbf{b}$, $\mathrm{Im}(C') \subseteq \mathrm{Im}(D)$, where Im() returns the image of a matrix. As D can be presented as an identity matrix, this condition is satisfied.

(4) Solution to each ADMM sub-problem is Lipschitz continuous. The details can be found in the assumption A3 in [40].

As the proposed ADMM model in local trading level satisfies all the conditions listed above, the convergence is proved. The proof process is also applicable to the regional trading level, as the objective function in the regional trading level (*i.e.* expression (25)) has the similar form to that in the local trading level.

Appendix B. Power flow models

(1) Newton–Raphson model

The Newton–Raphson model is developed based on the power balance equations as shown in expressions (40) and (41). The unknown voltage angle and magnitude values are updated through the iterations based on expressions (42) and (43), and the iterative process stops when the stopping conditions are satisfied.

$$\Delta P_i = -P_i + \sum_{j=1}^{n} v_i v_j\left(G_{ij}\cos(\theta_i - \theta_j) + B_{ij}\sin(\theta_i - \theta_j)\right) \tag{40}$$

$$\Delta Q_i = -Q_i + \sum_{j=1}^{n} v_i v_j\left(G_{ij}\sin(\theta_i - \theta_j) - B_{ij}\cos(\theta_i - \theta_j)\right) \tag{41}$$

$$\begin{bmatrix}\Delta \boldsymbol{v}\\ \Delta \boldsymbol{\theta}\end{bmatrix} = -\boldsymbol{J}^{-1}\begin{bmatrix}\Delta \mathbf{P}\\ \Delta \mathbf{Q}\end{bmatrix}, \quad \boldsymbol{J} = \begin{bmatrix}\frac{\Delta \mathbf{P}}{\Delta \boldsymbol{v}} & \frac{\Delta \mathbf{P}}{\Delta \boldsymbol{\theta}}\\ \frac{\Delta \mathbf{Q}}{\Delta \boldsymbol{v}} & \frac{\Delta \mathbf{Q}}{\Delta \boldsymbol{\theta}}\end{bmatrix} \tag{42}$$

$$\begin{bmatrix}\boldsymbol{v}\\ \boldsymbol{\theta}\end{bmatrix}^{k+1} = \begin{bmatrix}\boldsymbol{v}\\ \boldsymbol{\theta}\end{bmatrix}^{k} + \begin{bmatrix}\Delta \boldsymbol{v}\\ \Delta \boldsymbol{\theta}\end{bmatrix} \tag{43}$$

where P_i and Q_i are the active and reactive power injections at the ith node, respectively; v_i and θ_i are the voltage magnitude and phase angle at the ith node, respectively; G_{ij}, B_{ij} are the real part and imaginary part of the element in the bus admittance matrix, respectively; $\mathbf{P}, \mathbf{Q}, \boldsymbol{v}, \boldsymbol{\theta}$ are the corresponding vectors of nodal active and reactive power injections, voltage magnitude and phase angle, respectively; and $\boldsymbol{J}$ is the Jacobian matrix.

(2) DistFlow model

The DistFlow model was proposed for radial distribution networks by Baran and Wu in 1989. It is based on a set of simple, recursive equations known as forward DistFlow branch equations (as shown in expressions (44), (45) and (46)).

$$\sum_{(i,j)\in\Omega_L} P_{i,j}^{L} = \sum_{(j,i)\in\Omega_L}(P_{j,i}^{L} - \mathrm{r}_{j,i}I_{i,j}^2) + P_i^{G} - \mathrm{P}_i^{D} \tag{44}$$

$$\sum_{(i,j)\in\Omega_L} Q_{i,j}^{L} = \sum_{(j,i)\in\Omega_L}(Q_{j,i}^{L} - \mathrm{x}_{j,i}I_{i,j}^2) + Q_i^{G} - \mathrm{Q}_i^{D} \tag{45}$$

$$v_i^2 = v_j^2 - 2(\mathrm{r}_{i,j}P_{i,j}^{L} + \mathrm{x}_{i,j}Q_{i,j}^{L}) + (\mathrm{r}_{i,j}^2 + \mathrm{x}_{i,j}^2)I_{i,j}^2 \tag{46}$$

where P_{ij}^{L}, Q_{ij}^{L} and I_{ij}^{L} are the active power, reactive power and current on the line from the ith node to the jth node, respectively; P_i^{G}, P_i^{D}, Q_i^{G} and Q_i^{D} are the active generation, active demand, reactive generation and reactive demand at the ith node, respectively; and $r_{j,i}$ and $x_{j,i}$ are the resistance and reactance on the line from the ith node to the jth node, respectively.

Appendix C. Profit allocation in the bi-level TA network

(1) Profit allocation of local trading level in the TA mode

Considering the service charging from the local trading manager, the profit increase of the kth entity in the ith local community can be expressed as follows:

$$\Delta C_{ik}^{t}(TA_l)=\begin{cases}\left(1-\gamma_{li}\right)\frac{profit_i^t}{2}\frac{P_{ik}^t}{\sum_{k=1}^{n_{ef}}max\left(P_{ik}^t,0\right)}, & P_{ik}^t\geq 0\\ \left(1-\gamma_{li}\right)\frac{profit_i^t}{2}\frac{P_{ik}^t}{\sum_{k=1}^{n_{ef}}min\left(P_{ik}^t,0\right)}, & P_{ik}^t<0\end{cases} \tag{47}$$

where γ_{li} represents the service charging percentage of the ith local trading manager m_i. $profit_i^t$ is the negative value of the optimized result for the ith community (*i.e.*, $-f_i\left(\boldsymbol{x}_i\right)$) in the local trading level community formation model. The load of the entire community sent to the utility grid is P_i^t:

$$P_i^t=\sum_{k=1}^{n_{ef}}max\left(P_{ik}^t,0\right)+\sum_{k=1}^{n_{ef}}min\left(P_{ik}^t,0\right) \tag{48}$$

(2) Profit allocation of regional trading level in the TA mode

Similar to the calculation of $\Delta C_{ik}^t(TA_l)$, the profit increase of the qth regional entity in the pth regional community is expressed as:

$$\Delta C_{pq}^{t}(TA_r)=\begin{cases}\left(1-\gamma_{rp}\right)\frac{Profit_p^t}{2}\frac{P_{pq}^t}{\sum_{q=1}^{N_E}max\left(P_{pq}^t,0\right)}, & P_{pq}^t\geq 0\\ \left(1-\gamma_{rp}\right)\frac{Profit_p^t}{2}\frac{P_{pq}^t}{\sum_{q=1}^{N_E}min\left(P_{pq}^t,0\right)}, & P_{pq}^t<0\end{cases} \tag{49}$$

where γ_{rp} represents the service charging percentage of the pth regional trading manager. The cost of each regional entity C_{pq}^t is determined:

$$C_{pq}^t(TA)=p_s^t max\left(P_{pq}^t,0\right)+p_b^t min\left(P_{pq}^t,0\right)-\Delta C_{pq}^t(TA_r) \tag{50}$$

The load of the entire regional community sent to the utility grid is:

$$P_p^t=\sum_{q=1}^{N_E}max\left(P_{pq}^t,0\right)+\sum_{q=1}^{N_E}min\left(P_{pq}^t,0\right) \tag{51}$$

From the regional trading, the local manager m_i also gets extra profit increase $\Delta C_{pi}^t(TA_r)$. m_i will allocate $\Delta C_{pi}^t(TA_r)$ to the related local entities in the community as follows:

$$\Delta C_{ik}^{t}(TA_r)=\begin{cases}\left(1-\gamma_{li}\right)\Delta C_{pi}^t(TA_r)\frac{max\left(P_{ik}^t,0\right)}{\sum_{k=1}^{n_{ef}}max\left(P_{ik}^t,0\right)}, & P_i^t\geq 0\\ \left(1-\gamma_{li}\right)\Delta C_{pi}^t(TA_r)\frac{min\left(P_{ik}^t,0\right)}{\sum_{k=1}^{n_{ef}}min\left(P_{ik}^t,0\right)}, & P_i^t<0\end{cases} \tag{52}$$

It should be noted that only the local entities who make contributions will get extra profit. This means only one group between the selling entities and the local buying entities in a specific local community will earn profit from the regional trading. Then the total cost of each entity can be modified as follows:

$$\begin{aligned}C_{ik}^t(TA)=&p_s^t max\left(P_{ik}^t,0\right)+p_b^t min\left(P_{ik}^t,0\right)\\ &-\Delta C_{ik}^t(TA_l)-\Delta C_{ik}^t(TA_r)\end{aligned} \tag{53}$$

For some entities, they may only take part in the local level trading, and then the corresponding $\Delta C_{ik}^t(TA_r)$ is equal to zero in that case.

Appendix D. Profit allocation in the bi-level TPA mode

(1) Profit allocation of local trading level in the TPA mode

The profit increase of the kth entity in the ith local community in the TPA mode can be expressed as:

$$\Delta C_{ik}^{t}(TPA_l)=\begin{cases}\left(1-\delta_{li}\right)\frac{profit_i^t}{2}\frac{\sum_{j\in seller_k}V_{ikj}^t}{V_i^t}, & P_{ik}^t\geq 0\\ \left(1-\delta_{li}\right)\frac{profit_i^t}{2}\frac{\sum_{j\in buyer_k}V_{ikj}^t}{V_i^t}, & P_{ik}^t<0\end{cases} \tag{54}$$

where δ_{li} represents the service charging percentage of the local community manager in the P2P mode, which is much less than the service fee in the agent-based mode; and V_{ikj}^t is the trading volume between entity k and entity j in the ith community.

The load of the entire community sent to the utility grid is the total power output or demand which is not traded in the local P2P trading network. It is denoted by $P_{i\_non}^t$ and can be determined as follows:

$$P_{i\_non}^t=\sum_{k=1}^{n_{ef}}max\left(P_{ik\_non}^t,0\right)+\sum_{k=1}^{n_{ef}}min\left(P_{ik\_non}^t,0\right) \tag{55}$$

(2) Profit allocation of regional trading level in the TPA mode

The profit increase of the qth regional entity in the pth regional community in the TPA mode is:

$$\Delta C_{pq}^{t}(TPA_r)=\begin{cases}\left(1-\delta_{rp}\right)\frac{Profit_p^t}{2}\frac{\sum_{r\in seller_q}V_{qr}^t}{V_p^t}, & P_{pq}^t\geq 0\\ \left(1-\delta_{rp}\right)\frac{Profit_p^t}{2}\frac{\sum_{r\in buyer_q}V_{qr}^t}{V_p^t}, & P_{pq}^t<0\end{cases} \tag{56}$$

where δ_{rp} represents the service charging percentage of the regional manager p, and V_{qr}^t is the trading volume between regional entity q and r. Then, the cost of each regional entity taking part in the regional P2P trading is C_{pq}^t:

$$\begin{aligned}C_{pq}^t(TPA)=&p_s^t max\left(P_{pq}^t,0\right)+p_b^t min\left(P_{pq}^t,0\right)\\ &-\Delta C_{pq}^t(TPA_r)\end{aligned} \tag{57}$$

The load of the entire regional community sent to the utility grid is the total power output or demand which is not traded in the regional P2P trading network, denoted by $P_{p\_non}^t$:

$$P_{p\_non}^t=\sum_{q=1}^{N_E}max\left(P_{pq\_non}^t,0\right)+\sum_{q=1}^{N_E}min\left(P_{pq\_non}^t,0\right) \tag{58}$$

From the P2P trading at the regional level, the local manager m_i also gets extra profit increase ΔC_{pi}^t. m_i allocates ΔC_{pi}^t to the related local entities in the community.

$$\Delta C_{ik}^{t}(TPA_r)=\begin{cases}\left(1-\gamma_{li}\right)\Delta C_{pi}^t(TPA)\frac{max\left(P_{ik\_non}^t,0\right)}{\sum_{k=1}^{n_{ef}}max\left(P_{ik\_non}^t,0\right)}, & P_{i\_non}^t\geq 0\\ \left(1-\gamma_{li}\right)\Delta C_{pi}^t(TPA)\frac{min\left(P_{ik\_non}^t,0\right)}{\sum_{k=1}^{n_{ef}}min\left(P_{ik\_non}^t,0\right)}, & P_{i\_non}^t<0\end{cases} \tag{59}$$

Similarly, only the local entities which make contributions will get the extra profit. Then the total cost of each local entity will be modified as follows:

$$\begin{aligned}C_{ik}^t(TPA)=&p_s^t max\left(P_{ik}^t,0\right)+p_b^t min\left(P_{ik}^t,0\right)\\ &-\Delta C_{ik}^t(TPA_l)-\Delta C_{ik}^t(TPA_r)\end{aligned} \tag{60}$$

Appendix E. Complex network indices for trading networks

(1) Node degree: the degree of a node is defined as its number of connections to other nodes, and the degree distribution is the probability distribution of these degrees. Considering degree k of a node in graph G is a random variable, the function N_k is the node degree distribution [25]:

$$N_k=\{v\in G:d(v)=k\} \tag{61}$$

where N_k is the number of nodes with node degree k. Average degree (AD) is defined as the average of all nodes' degrees, and average weighted degree (AWD) is the average of the connected edges' weights of all nodes.

(2) Modularity index [41]: many networks consist of distinct "communities", which means the connections of vertices within community are dense but they are sparser between communities. The modularity index can evaluate how good the community structures are. It is defined as the fraction of edges that fall within communities minus the expected value of the same quantity if edges are assigned at random. The modularity Q can be expressed as:

$$Q = \frac{1}{2m} \sum_{ij} \left[(A_{ij} - \frac{k_i k_j}{2m}) \delta(c_i, c_j) \right] \tag{62}$$

where m is the total number of edges in the graph, A is the adjacency matrix, k_i and k_j are the degrees of vertex i and vertex j, c_i and c_j are the communities to which vertex i and vertex j is assigned respectively. $\delta(u, v) = 1$ if $u = v$, otherwise $\delta(u, v) = 0$.

(3) Average path length (APL) [42]: APL is defined as the average number of steps along the shortest paths for all possible pairs of network nodes:

$$L_A = \frac{1}{n(n-1)} \sum_{i \neq j} l(i, j) \tag{63}$$

where n is the total number of nodes in a graph; $l(i, j)$ denotes the shortest distance between i and vertex j.

(4) Average clustering coefficient (ACC) [25]: ACC is defined as the average of all nodes' clustering coefficients, which is a measure of the degree to which the nodes in a graph tend to cluster together. The clustering coefficient of a node v is calculated as follows:

$$\gamma_v = \frac{|E(\Gamma_v)|}{\binom{k_v}{2}} \tag{64}$$

where Γ_v is the neighborhood of vertex v, *i.e.*, the set of vertices adjacent to vertex v, $|E(\Gamma_v)|$ is the number of edges in Γ_v, $\binom{k_v}{2}$ is the total number of possible edges in Γ_v.

(5) Density [43]: density is defined as the ratio of the number of edges to the number of possible edges in a graph:

$$\rho = \frac{2m}{n(n-1)} \tag{65}$$

Appendix F. Link entropy index for communication network

The LE index [44] is used to represent the edge significance on maintaining the global connectivity of the communication network in this paper. The LE index was devised considering two types of important edges, including the edges linked with overlapping nodes and the edges between obviously different communities. The information entropy and Jensen–Shannon divergence indices are utilized accordingly to reflect these two types of edges in the LE index model, which can be expressed as:

$$LE_{ij} = \frac{\frac{H(L_i)+H(L_j)}{2} + JSD\left(\boldsymbol{L}_i \parallel \boldsymbol{L}_j\right)}{2} \tag{66}$$

where $\boldsymbol{L}_i$ is the probability distribution vector of node i, $H\left(\boldsymbol{L}_i\right)$ is the information entropy of node i, and $JSD\left(\boldsymbol{L}_i \parallel \boldsymbol{L}_j\right)$ is the Jensen–Shannon divergence of $\boldsymbol{L}_i$ and $\boldsymbol{L}_j$.

$$H\left(\boldsymbol{L}_i\right) = -\sum_{k=1}^{K} l_{ik} log(l_{ik}) \tag{67}$$

$$JSD(\boldsymbol{L}_i \parallel \boldsymbol{L}_j) = \frac{1}{2} D(\boldsymbol{L}_i \parallel \boldsymbol{M}) + \frac{1}{2} D(\boldsymbol{L}_j \parallel \boldsymbol{M}) \tag{68}$$

$$\boldsymbol{M} = \frac{1}{2}\left(\boldsymbol{L}_i + \boldsymbol{L}_j\right), \tag{69}$$

$$D(\boldsymbol{L}_i \parallel \boldsymbol{M}) = \sum_{k=1}^{K} l_{ik} log \frac{l_{ik}}{m_k} \tag{70}$$

It is assumed that the pairwise interactions described in the adjacency matrix $\boldsymbol{A}$ are influenced by an unobserved expectation network $\widehat{\boldsymbol{A}}$. Here we define l_{ik} as the probability that node i belongs to community k, and m_k is the kth element in $\boldsymbol{M}$. So an expected edge $\widehat{a_{ij}}$ can be estimated as:

$$\widehat{a_{ij}} = \sum_{k=1}^{K} l_{ik} l_{jk} \tag{71}$$

$$\widehat{\boldsymbol{A}} = \boldsymbol{L}\boldsymbol{L}^T \tag{72}$$

A square loss function is adopted here to measure the difference between the observed matrix $\boldsymbol{A}$ and the expected matrix $\widehat{\boldsymbol{A}}$, and l_{ik} can be determined through the following optimization problem:

$$\boldsymbol{L} = \underset{L \geq 0}{\mathbf{argmin}} \left\| \boldsymbol{A} - \widehat{\boldsymbol{A}} \right\| \tag{73}$$

References

[1] Foumani M, Smith-Miles K. The impact of various carbon reduction policies on green flowshop scheduling. Appl Energy 2019;249:300–15.

[2] Bremdal BA, Olivella P, Rajasekharan J. EMPOWER: A network market approach for local energy trade. In: PowerTech, 2017 IEEE Manchester. IEEE; 2017, p. 1–6.

[3] Luo F, Dong ZY, Liang G, Murata J, Xu Z. A distributed electricity trading system in active distribution networks based on multi-agent coalition and blockchain. IEEE Trans Power Syst 2018.

[4] Chen T, Su W. Indirect customer-to-customer energy trading with reinforcement learning. IEEE Trans Smart Grid 2018.

[5] Pagani GA, Aiello M. Power grid network evolutions for local energy trading. 2012, arXiv preprint arXiv:1201.0962.

[6] Mengelkamp E, Notheisen B, Beer C, Dauer D, Weinhardt C. A blockchain-based smart grid: towards sustainable local energy markets. Comput Sci Res Dev 2018;33(1–2):207–14.

[7] Mengelkamp E, Gärttner J, Rock K, Kessler S, Orsini L, Weinhardt C. Designing microgrid energy markets: A case study: The Brooklyn Microgrid. Appl Energy 2018;210:870–80.

[8] Pilz M, Al-Fagih L. Recent advances in local energy trading in the smart grid based on game-theoretic approaches. IEEE Trans Smart Grid 2017;10(2):1363–71.

[9] Wu Y, Tan X, Qian L, Tsang DH, Song W-Z, Yu L. Optimal pricing and energy scheduling for hybrid energy trading market in future smart grid. IEEE Trans Ind Inf 2015;11(6):1585–96.

[10] Tushar W, Saha TK, Yuen C, Morstyn T, Poor HV, Bean R, et al. Grid influenced peer-to-peer energy trading. IEEE Trans Smart Grid 2019.

[11] Parag Y, Sovacool BK. Electricity market design for the prosumer era. Nature Energy 2016;1(4):1–6.

[12] Sorin E, Bobo L, Pinson P. Consensus-based approach to peer-to-peer electricity markets with product differentiation. IEEE Trans Power Syst 2018;34(2):994–1004.

[13] Liu N, Yu X, Wang C, Li C, Ma L, Lei J. Energy-sharing model with price-based demand response for microgrids of peer-to-peer prosumers. IEEE Trans Power Syst 2017;32(5):3569–83.

[14] Ma L, Liu N, Zhang J, Wang L. Real-time rolling horizon energy management for the energy-hub-coordinated prosumer community from a cooperative perspective. IEEE Trans Power Syst 2018;34(2):1227–42.

[15] Chiş A, Koivunen V. Coalitional game-based cost optimization of energy portfolio in smart grid communities. IEEE Trans Smart Grid 2017;10(2):1960–70.

[16] Sousa T, Soares T, Pinson P, Moret F, Baroche T, Sorin E. Peer-to-peer and community-based markets: A comprehensive review. Renew Sustain Energy Rev 2019;104:367–78.

[17] Paudel A, Chaudhari K, Long C, Gooi HB. Peer-to-peer energy trading in a prosumer-based community microgrid: A game-theoretic model. IEEE Trans Ind Electron 2018;66(8):6087–97.

[18] Tushar W, Yuen C, Mohsenian-Rad H, Saha T, Poor HV, Wood KL. Transforming energy networks via peer to peer energy trading: Potential of game theoretic approaches. 2018, arXiv preprint arXiv:1804.00962.

[19] LO3 energy: The future of energy. 2018, [Online]. Available: https://lo3energy.com/.

[20] Khorasany M, Mishra Y, Ledwich G. Market framework for local energy trading: a review of potential designs and market clearing approaches. IET Gen Transm Distrib 2018;12(22):5899–908.

[21] Moret F, Pinson P. Energy collectives: a community and fairness based approach to future electricity markets. IEEE Trans Power Syst 2018;34(5):3994–4004.

[22] Saad W, Han Z, Poor H. Coalitional game theory for cooperative micro-grid distribution networks. In: 2011 IEEE International conference on communications workshops. IEEE; 2011, p. 1–5.

[23] Ni J, Ai Q. Economic power transaction using coalitional game strategy in micro-grids. IET Gen Transm Distrib 2016;10(1):10–8.
[24] Notice on carrying out the pilot project of marketized trading in distributed generation. 2017, [Online]. Available: http://zfxxgk.nea.gov.cn/auto87/201711/t20171113_3055.htm.
[25] Pagani GA, Aiello M. The power grid as a complex network: a survey. Physica A 2013;392(11):2688–700.
[26] Jiang Z, Wang L, Chen W. A distribution network islanding strategy based on topological characteristics to improve system resiliency. In: 2018 2nd IEEE conference on energy internet and energy system integration. IEEE; 2018, p. 1–6.
[27] Alam M, St-Hilaire M, Kunz T. Peer-to-peer energy trading among smart homes. Appl Energy 2019;238:1434–43.
[28] Hausheer D. PeerMart: Secure decentralized pricing and accounting for peer-to-peer systems. ETH Zurich; 2006.
[29] Boyd S, Parikh N, Chu E, Peleato B, Eckstein J, et al. Distributed optimization and statistical learning via the alternating direction method of multipliers. Found Trends® Mach Learn 2011;3(1):1–122.
[30] Wu B, Ghanem B. lp-box ADMM: A versatile framework for integer programming. IEEE Trans Pattern Anal Mach Intell 2018;41(7):1695–708.
[31] Arianos S, Bompard E, Carbone A, Xue F. Power grid vulnerability: A complex network approach. Chaos 2009;19(1):013119.
[32] Grainger JJ, Stevenson WD. Power system analysis. Singapore: McGraw-Hill; 1994.
[33] Baran ME, Wu FF. Optimal capacitor placement on radial distribution systems. IEEE Trans Power Deliv 1989;4(1):725–34.
[34] Zhang Z, Li R, Li F. A novel peer-to-peer local electricity market for joint trading of energy and uncertainty. IEEE Trans Smart Grid 2019. 1–1.
[35] Schleicher-Tappeser R. How renewables will change electricity markets in the next five years. Energy Policy 2012;48:64–75.
[36] Zhang C. Peer-to-peer energy trading in electrical distribution networks [Ph.D. dissertation], Cardiff University; 2017.
[37] Morstyn T, Farrell N, Darby SJ, McCulloch MD. Using peer-to-peer energy-trading platforms to incentivize prosumers to form federated power plants. Nature Energy 2018;3(2):94–101.
[38] Bayram IS, Shakir MZ, Abdallah M, Qaraqe K. A survey on energy trading in smart grid. In: 2014 IEEE global conference on signal and information processing. IEEE; 2014, p. 258–62.
[39] Zhou Y, Wu J, Long C. Evaluation of peer-to-peer energy sharing mechanisms based on a multiagent simulation framework. Appl Energy 2018;222:993–1022.
[40] Wang Y, Yin W, Zeng J. Global convergence of ADMM in nonconvex nonsmooth optimization. J Sci Comput 2019;78(1):29–63.
[41] Newman ME. Analysis of weighted networks. Phys Rev E 2004;70(5):056131.
[42] Albert R, Barabási A-L. Statistical mechanics of complex networks. Rev Modern Phys 2002;74(1):47.
[43] Wasserman S, Faust K, et al. Social network analysis: Methods and applications, vol. 8. Cambridge University Press; 1994.
[44] Qian Y, Li Y, Zhang M, Ma G, Lu F. Quantifying edge significance on maintaining global connectivity. Sci Rep 2017;7:45380.